

NUMERICAL IMPACT DAMAGE MODELLING IN COMPOSITE STRUCTURES USING STRAIN RATE DEPENDENT CONSTITUTIVE MODELS

J. Ratković^{1*} and D. Ivančević²

¹ Department of Technology, Faculty of Mechanical Engineering and Naval Architecture, University of Zagreb, Zagreb, Croatia

² Department of Aeronautical Engineering, Faculty of Mechanical Engineering and Naval Architecture, University of Zagreb, Zagreb, Croatia

* Corresponding author (jakov.ratkovic@fsb.hr)

Keywords: Impact damage, Damage mechanics, Strain-rate dependent failure theory

ABSTRACT

The present work deals with constitutive modelling of the impact response of woven carbon fibre reinforced polymer composites. A modification of the previously developed VUMAT Fortran subroutine prepared for utilization in combination with *Abaqus/Explicit* is presented. The previously developed model for unidirectional plies is now extended to utilization in the case of woven plies as well. Strain rate dependence of ply strength values is implemented using logarithmic functions, with a low-pass filter smoothing of numerically obtained strain rate values. Failure initiation is modelled according to the modified Hashin's theory consisting of a total of five failure criteria. Validation of the developed constitutive model is performed by comparison of numerical results to the numerical and experimental data available in the researched literature. Results have demonstrated that the constitutive model at the current state has a capability to capture low impact energy phenomena accurately. They have also shown that the future work proposed in this paper should lead to improvements in the accuracy of the impact numerical simulation predictions in wide range of velocities, i.e. impact energies.

1. INTRODUCTION

Impact damage is a specific concern in laminated composite structures due to the inherent heterogeneity of the material at various length scales. The structural behavior during the impact event is even more complicated since carbon fiber composites exhibit significant strain-rate dependence of the elasticity and strength properties as documented in e.g. [1].

Numerical techniques are increasingly being used in the design process of state-of-the-art automotive and aerospace structures where crashworthiness is one of the key design criteria. To improve accuracy and reliability of the impact damage procedures, this work presents a numerical methodology that is focused on unidirectional (UD) and woven composite plies at a wide range of impact velocities and strain rates. Previously developed and tested for UD composites, the existing model represents an adequate base for further development of the material constitutive model suitable for woven composite plies.

Based on the available references, it can be concluded that in research generally woven composites are significantly less covered compared to the unidirectional composites [2]. By incorporating certain assumptions, in specific cases, the UD lamina theories can be utilized for woven composites as well. The major issue in this approach lays in the nature of the woven material itself – the fibers are placed in both directions (warp and weft) of the lamina plane and are more interconnected.

Most of the UD ply failure theories consist of four different failure criteria corresponding to fiber and matrix tensile and compressive failure [2]. Therefore, the simple starting point approach is to utilize the two (tensile and compressive) failure criteria developed for fiber direction in UD plies for modelling of all four in-plane failure modes - warp and weft compressive and tensile failure modes in woven plies. Additionally, existence of resin rich zones has a significant impact on the woven lamina behavior that has to be accounted for in numerical procedures [3]. Finally, woven lamina exhibits, especially in the high strain rate conditions such as impact loading regimes, a pronounced non linear behaviour [4] specifically characteristic for shear directions.

In this work, a starting point of the development of the woven CFRP strain rate dependent constitutive model is presented, by means of incorporating the appropriate failure criteria and including the strain rate effects partially - i.e. the strain rate dependence of the ply strength values. The model is validated against existing experimental results by performing ballistic impact simulations on CFRP rectangular plate. Further work agenda is briefly presented, including damage propagation laws and delamination modelling.

2. METHODOLOGY

The strain rate effects have been implemented using the VUMAT subroutine that allows user-defined definition of the constitutive relations in *Abaqus/Explicit*. In the original code, the phenomenological-based theory, introduced in [5], has been selected as the damage initiation criterion. The model is based on Puck's theory that has been modified to include the strain rate effects. Consequently, logarithmic functions have been used to include the strain rate effects by scaling the strength values.

2.1. Strain rate dependency

As it was already mentioned, it is a known fact that increased strain rate leads to elevation of CFRP strength values. Therefore, according to [5], a logarithmic function is utilized to model this dependency law as follows:

$$k_{ii}(\dot{\epsilon}_{ii}) = K_0 + K_1 \cdot \log(|\dot{\epsilon}_{ii}|) + K_2 \cdot (\log(|\dot{\epsilon}_{ii}|))^2, \quad (1)$$

where K_0 , K_1 and K_2 are the curve fitting parameters used to determine the $k_{ii}(\dot{\epsilon}_{ii})$ strain rate effect parameter corresponding to strain rate $\dot{\epsilon}_{ii}$ and strength in the direction ii . As could be seen from material strength data given in Table 1, taken from [6] for a material system T300 K3/IMP530R and T300 K12/IMP530R, it is evident that the increase of strength value in the elevated strain rate conditions is varying for different strengths. Hence, different curve fitting parameters are established for separate strengths. Values of fitting parameters K_0 and K_1 corresponding to specific strengths of the used material system utilized in this work are shown in Table 1 as well. Values of K_2 fitting parameters were set to zero for strengths in all directions.

Parameter	Unit	Quasi-static	Dynamic	K_0 , [-]	K_1 , [-]
$X_t = Y_t$	[MPa]	52	594.2	1.07	0.024
$X_c = Y_c$	[MPa]	471.2	849.4	1.40	0.134
Z_t	[MPa]	73	107.8	1.24	0.079
Z_c	[MPa]	320.1	348.6	1.04	0.016
$S_{12} = S_{23} = S_{13}$	[MPa]	100	194.5	1.47	0.158

Table 1: Extrapolated quasi-static and dynamic strength data for a material system T300 K3/IMP530R, T300 K12/IMP530R [6,7], along with strain rate effects fitting parameters K_0 and K_1

Failure envelopes in the $\sigma_{11} - \sigma_{22}$ and $\sigma_{22} - \sigma_{12}$ plane for quasi-static (0.001 s^{-1}), elevated (1 s^{-1}) and high (1000 s^{-1}) strain rate conditions are depicted in Figure 1 a) and b) respectively, and are showing a good agreement with the strength data given in Table 1. As could be seen in the following section, shear strength increase with the elevation of strain rates is not taken into account in the proposed failure criteria.

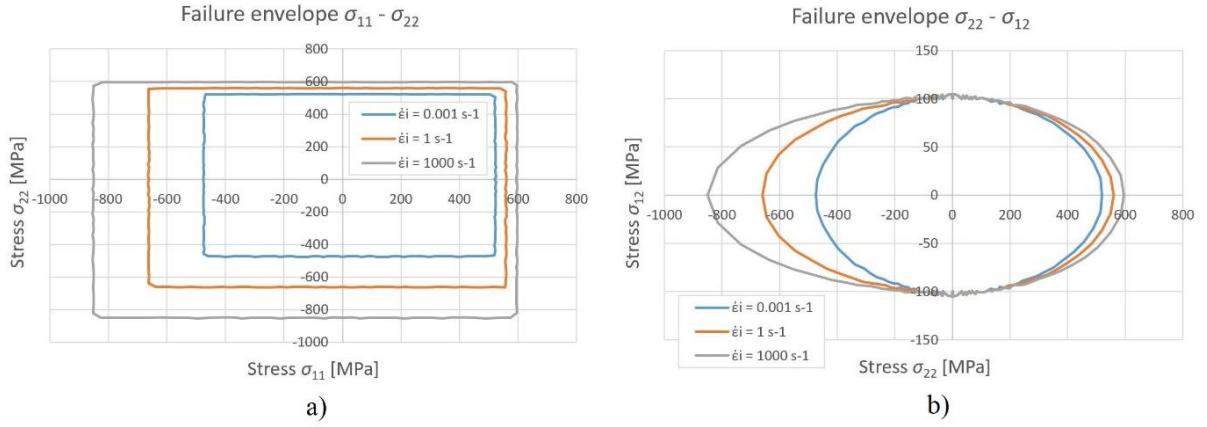


Figure 1: Failure envelopes for quasi-static (0.001 s^{-1}), elevated (1 s^{-1}) and high (1000 s^{-1}) strain rates:
a) in the $\sigma_{11} - \sigma_{22}$ plane, b) in the $\sigma_{22} - \sigma_{12}$ plane

It is of significant importance to address the solution to inherent strain-rate value oscillation that arises as a result of the explicit numerical integration scheme. In order to overcome this problem, as opposed to the frequently used simple averaging method, a low-pass filter is modelled as proposed in [8] and is implemented in the model. Utilization of the low-pass filter requires determination of two variables, namely threshold ($\Delta\dot{\epsilon}_{tsh}$) and limit ($\Delta\dot{\epsilon}_{lim}$) values of strain rate difference in a single simulation increment ($\Delta\dot{\epsilon}_t = \dot{\epsilon}_t - \dot{\epsilon}_{t-\Delta t}$). The strain rate increment $\Delta\dot{\epsilon}$ is evaluated by comparing it to the threshold value $\Delta\dot{\epsilon}_{tsh}$, and, if it is greater than the defined threshold, it must be reduced to a processed value $\Delta\dot{\epsilon}_{proc}$ according to the law presented by relation [8]:

$$\Delta\dot{\epsilon}_{proc} = \Delta\dot{\epsilon}_{tsh} + (\Delta\dot{\epsilon}_{lim} - \Delta\dot{\epsilon}_{tsh}) \cdot \left(1 - e^{-\frac{\Delta\dot{\epsilon} - \Delta\dot{\epsilon}_{tsh}}{\Delta\dot{\epsilon}_{lim} - \Delta\dot{\epsilon}_{tsh}}}\right). \quad (2)$$

2.2. Failure initiation

Failure initiation, in the case of woven plies, is modelled according to modified version of Hashin's failure theory presented in [6], which distinguishes eight different failure criteria: warp and weft fiber direction tensile and compressive criteria, three shear failure criteria and a single matrix failure initiation criterion. For the simplicity reasons, considering the fact that no damage propagation is included in the model, at this stage of the research the shear failure criteria are not implemented. The rest of the named criteria are respectively as follows:

$$FF1T = \left(\frac{\sigma_{11}}{X_t^d}\right)^2 + \left(\frac{\tau_{12}}{S_{12}}\right)^2 + \left(\frac{\tau_{13}}{S_{13}}\right)^2 \geq 1, \quad (3)$$

$$FF1C = \left(\frac{\sigma_{11}}{X_c^d}\right)^2 + \left(\frac{\tau_{12}}{S_{12}}\right)^2 + \left(\frac{\tau_{13}}{S_{13}}\right)^2 \geq 1, \quad (4)$$

$$FF2T = \left(\frac{\sigma_{22}}{Y_t^d}\right)^2 + \left(\frac{\tau_{12}}{S_{23}}\right)^2 + \left(\frac{\tau_{23}}{S_{23}}\right)^2 \geq 1, \quad (5)$$

$$FF2C = \left(\frac{\sigma_{22}}{Y_c^d}\right)^2 + \left(\frac{\tau_{12}}{S_{23}}\right)^2 + \left(\frac{\tau_{23}}{S_{23}}\right)^2 \geq 1, \text{ and} \quad (6)$$

$$\begin{aligned}
MFT = MFC = & \left(\frac{\sigma_{11}}{2 \cdot X_{t/c}^d} \right)^2 + \left(\frac{\sigma_{22}}{2 \cdot Y_{t/c}^d} \right)^2 + \left(\frac{\tau_{12}}{S_{12}} \right)^2 + \left(\frac{\tau_{23}}{S_{23}} \right)^2 + \left(\frac{\tau_{13}}{S_{13}} \right)^2 \\
& + \left(\frac{\sigma_{33}^2}{Z_t^d \cdot Z_c^d} \right) + \sigma_{33} \cdot \left(\frac{1}{Z_t^d} + \frac{1}{Z_c^d} \right) \geq 1.
\end{aligned} \tag{7}$$

As stated above and could be seen from eq. (7), a single matrix criterion is proposed. However, in order to be able to get better understanding and track the physical behaviour of the analyzed composite plate, it is convenient to simply separate the criterion to tensile and compressive ones, based on the sign of the stress component σ_{33} .

2.4. Numerical model

A numerical model identical to the one examined in [6,7] was created using *Abaqus/Explicit* finite element method software. A square composite panel of 195 x 195 mm² surface area and nominal thickness of 5.58 mm in a cantilever fixture is impacted by a solid 23.8 mm diameter steel spherical impactor of 54.7 g mass at various initial velocities. A ten-ply layup consisting of two outer (surface) plies of thickness of 0.31 mm and eight mid (bulking) plies of nominal thickness of 0.62 mm was used. All plies placed in the same orientation ($[0^\circ, 90^\circ]$), hence contributing to the assumption of orthotropic behaviour. For the CFRP material system used, extrapolated elastic properties obtained from [6] are shown in Table 2. The modelled assembly with boundary and initial conditions is depicted in Figure 2.

Elastic property	Unit	Value
$E_1 = E_2$	[GPa]	51
E_3	[GPa]	8
G_{12}	[GPa]	4.032
$G_{23} = G_{13}$	[GPa]	3
ν_{12}	[-]	0.06
$\nu_{23} = \nu_{13}$	[-]	0.3

Table 2: Extrapolated elastic properties for T300 K3/IMP530R and T300 K12/IMP530R material system [6]

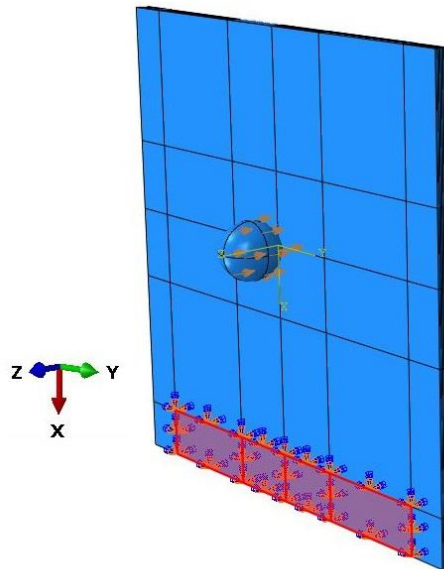


Figure 2: Numerical model with prescribed boundary and initial conditions

The impact event was analysed in three different conditions; three different impact energies - namely 96.8 J, 168.5 J and 229 J, corresponding to initial velocities of 59.5 m/s, 78.5 m/s and 91.5 m/s, respectively. The composite plate was numerically modelled by first order hexagonal finite elements with reduced integration (C3D8R). Each ply of the laminate was modelled by one finite element through the thickness. Varying size of finite elements was employed for the sake of computational efficiency - directly under the impactor, an approximate size of 1 mm of an element is used, while further away an average size of 2 mm is utilized. Steel projectile was modelled as a linearly elastic deformable body, described by the same type of finite elements of average size equal to 1 mm. Material properties used for the steel impactor are given in Table 3.

Property	Unit	Value
E	[GPa]	210
ν	[-]	0.3
ρ	[kg/m ³]	7750

Table 3: Steel impactor material properties

Mesh discretization of the numerical model is shown in Figure 3. The total number of finite elements for the composite plate is 163840, while the impactor was modelled by 12744 finite elements.

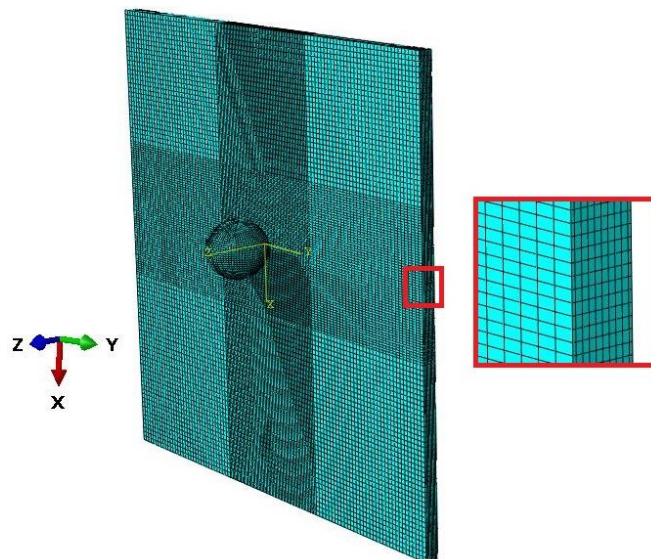


Figure 3: Meshed numerical model with a detail of the plate through thickness finite element discretization

3. RESULTS

One of the numerical difficulties in the modelling of impact phenomena using strain rate dependent constitutive models is the aforementioned spurious oscillation in the strain rates that are calculated from the explicit FE procedure. To obtain physically accurate and robust strain rates as input parameters for the constitutive models, several approaches have been tested. The result in Figure 4 shows the effect of the already named approach of using the low-pass filter. The strain rate in this result is the normal strain rate in the finite element at the impact location that has a very high value at the initial contact.

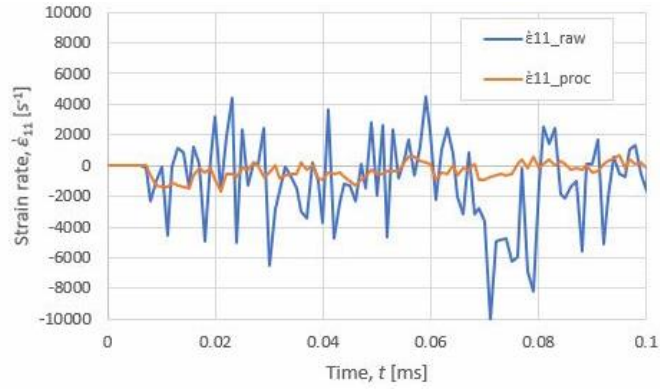


Figure 4: Raw and processed history of strain rate $\dot{\epsilon}_{11}$

Comparison of the out of plane displacements (u_z) along vertical and horizontal paths along the plate directly under the impactor are given in Figure 5 for the lowest impactor velocity analyzed (59.5 m/s), and in Figure 6 for the medium impactor velocity of 78.5 m/s, in various time sequences. In order to keep the results readable and concise, only 3/5 experimental time sequence curves per graph were displayed. Due to the lack of experimental data available in the work [6,7], results of the highest impact velocity were not analyzed in an analogous manner.

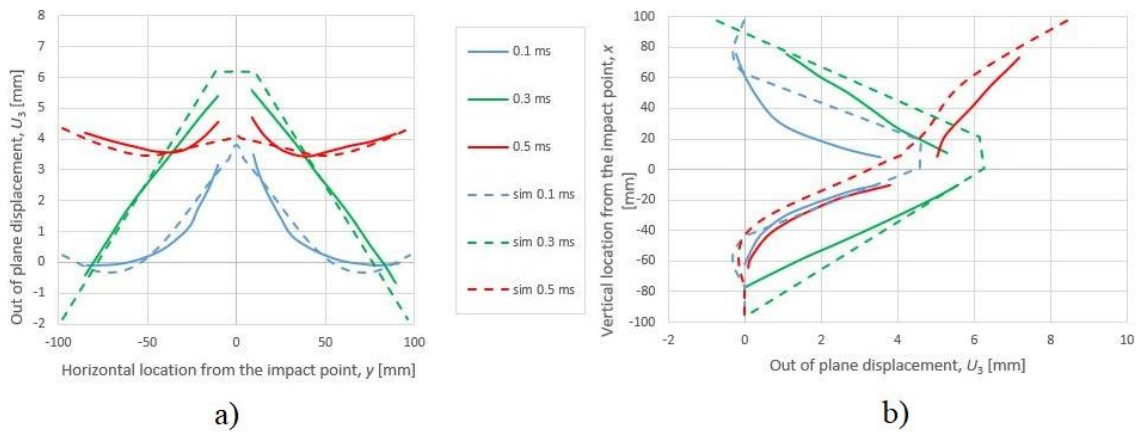


Figure 5: Out of plane displacement fields in low velocity impact: a) over horizontal path, b) over vertical path

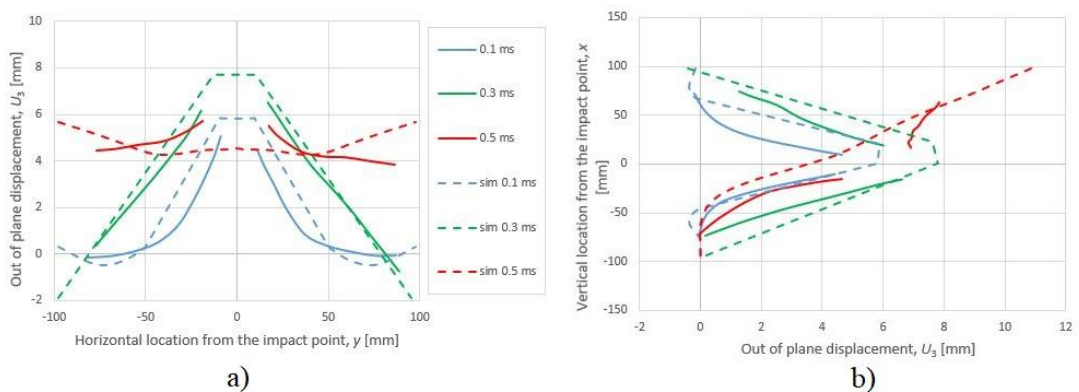


Figure 6: Out of plane displacement fields in mid velocity impact: a) over horizontal path, b) over vertical path

As could be seen from Figure 5, the herein developed model with purely elastic behaviour is correlating well with the experimentally obtained results from [6,7]. On the other hand, larger deviation could be observed from Figure 6 depicting the response of the plate in the case of the intermediate velocity impact. Some result discrepancies may originate from simple difference of the exact starting distance of the impactor, and thus time sequence selection differences. However, the main reason for the observed differences is known and is addressed in the following section.

Failure criteria values for the highest velocity impact are shown in Figure 7. In the figure, fiber tensile and compressive failure criteria for direction 1 (*FFIT* and *FFIC*) are presented along the matrix tensile (*MFT*) and compressive (*MFC*) criteria, over the plies 1, 4, 7 and 10. As the fiber failure criteria are identical in both in-plane directions (*I* and *2*), the failure index distributions are similar, hence the display of the *FF2T* and *FF2C* is left out.

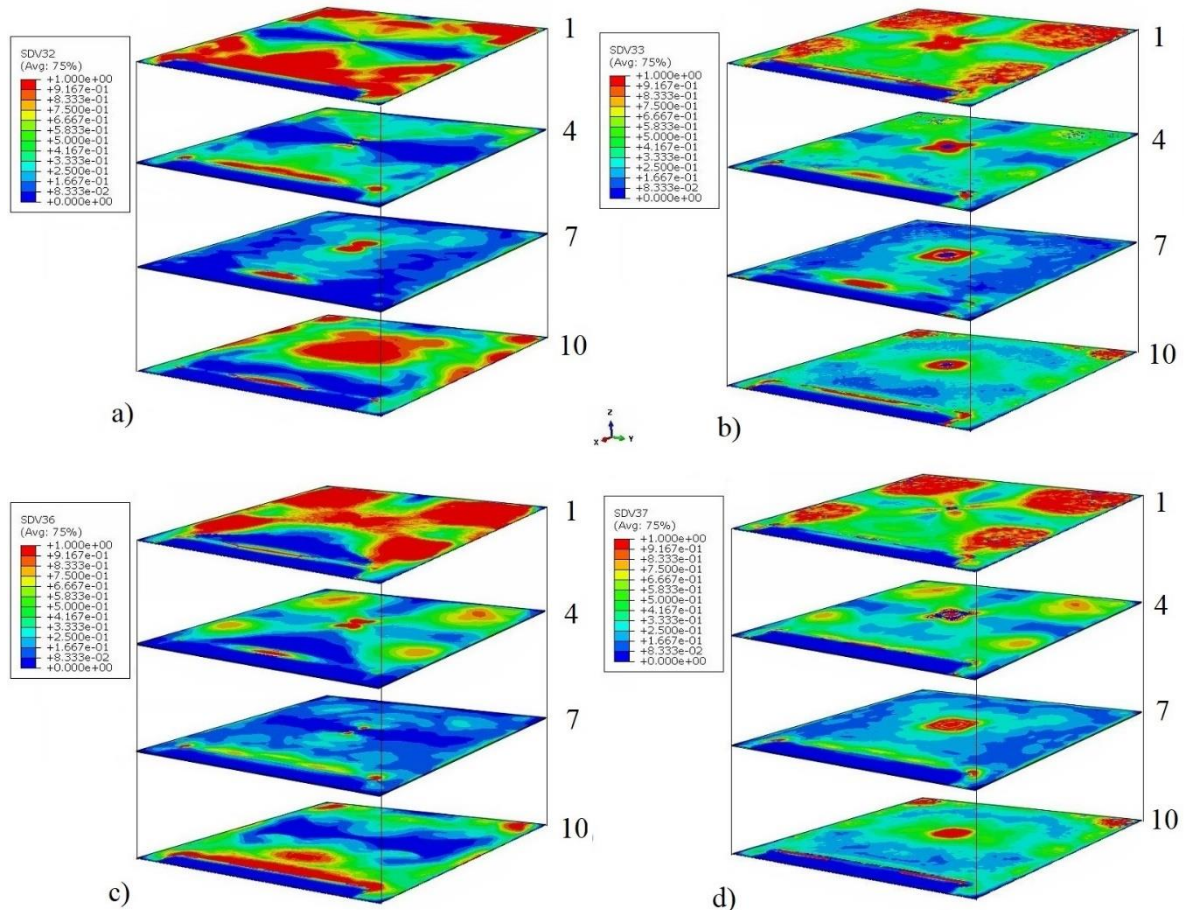


Figure 7: Failure criteria in different plies: a) *FFIT*, b) *FFIC*, c) *MFT*, d) *MFC*

Failure criteria displayed in Figure 7 contribute to understanding the validity of the constitutive model developed, and lead to the conclusion that the failure criteria and solution in general are physically sound. As expected, the tensile stresses leading to tensile fiber failure (Figure 7 a) occur in the upper plies further away from the impact point, and on the bottom plies in the zone of the impact (middle of the plate). On the other hand, compressive fiber failure (Figure 7 b) occurs in the center of the plate throughout the whole thickness. While observing the matrix tensile failure indexes (Figure 7 c), compared to fiber tensile failure, similar conclusions could be made. On the lower surface ply (ply 10), expected as well, tensile matrix failure is observed along the edge of the cantilever clamping fixture.

Unanticipated were only the compressive failure indications of both fiber and matrix in the remoted area of the exposed surface ply (ply 1). This phenomenon might need further investigation in future exercises.

4. DISCUSSION

It is evident that the observations found in the previous section mainly arise from the lack of the damage propagation mechanism in the developed model - the higher the impact energy (i.e. impact velocity) - the more damage is induced in the plate. Another significant difference that has an impact on the result discrepancy between the herein developed model and the reference model [6] is the lack of the existence of strain rate effects on the stiffness parameters in here proposed model. The reference model utilizes the identical logarithmic functions (with different fitting parameter values) for stiffness and strength strain rate dependency, as proposed in [10]. The theory [10] was previously researched by the authors and is still considered as a viable alternative for the implementation in the constitutive model code.

The research presented in this work is currently in the phase of implementation of a well-known damage evolution model implementation is in progress, by means of bilinear traction-separation law, utilizing five damage variables corresponding to the defined failure criteria. However, an interesting strain-rate dependent damage propagation model designated specifically for plain woven composites is proposed in [11] and is planned to be tested in the future with the here examined constitutive model.

Finally, an important further research phase is the implementation of an interply damage model that would enable modelling of delaminations. At this stage, the proposed model does not incorporate the delamination failure initiation and damage propagation model. However, delamination failure mode is generally known to be one of the most common, and in the case of impact loadings, most severe failure modes according to many resources and researches published, e.g. [12]. Thus, it is evident that better predictions of composite behaviour in various conditions require specific attention paid to delamination modelling. Future work includes modelling delamination behaviour according to [13].

5. CONCLUSIONS

In this work, introduction to the current stage of work in progress, by means of developing a woven CFRP strain rate dependent constitutive model with a rate dependent failure initiation theory is presented. At this stage, the constitutive model expansion from unidirectional to woven ply laminate has been made, including failure criteria modification and strain rate effects inclusion, and has been proved to be successful.

By the out of plane displacement results compared to experimentally obtained ones presented in the paper, as expected, it is obvious that pure linear elastic material response fails to provide a good prediction in the case of elevated impact energies. Failure criteria distribution over different plies provides adequate evidence of logical and physically sound behaviour of the developed model and also points to specific results that may require further investigation.

Further work considerations consist of more detailed strain-rate effects implementation - regarding the linkage of increase of stiffness parameters and possibly fracture toughness with the increase of strain rates. Furthermore, advanced damage evolution laws implementation and more sophisticated failure initiation criteria may lead to better load bearing capability prediction for woven composites, especially in the case of impact damage evaluation. The non-linearity of the shear response will be incorporated as well, by modelling the constitutive relations according to [4]. Last but not least, introduction of delamination failure mode initiation and propagation in the constitutive material model is from author's perspective the most significant advancement to be made to the current model, in order to obtain more accurate simulation results, and thus more high-fidelity solutions.

ACKNOWLEDGEMENTS

The research is fully funded by the Croatian Science Foundation (HRZZ) within the project "Computational Modelling of Composite Structures Impact Damage" (CONCORDE), grant number UIP-HRZZ-2020-02-9317.

REFERENCES

- [1] H. Koerber and P.P. Camanho, High strain rate characterization of unidirectional carbon epoxy IM7-8552 in longitudinal compression, *Composites: Part A*; Vol. 42(5), 2011, pp. 462-470, (doi: 10.1016/j.compositesa.2011.01.002).
- [2] M. H. Kashani and A. S. Milani, Damage Prediction in Woven and Non-woven Fabric Composites, In *Non-woven Fabrics*, InTechOpen: Rijeka, Croatia, 2016, pp. 223–262.
- [3] I. K. Giannopoulos, M. Yasaee, and N. Maropakis, Ballistic Impact and Virtual Testing of Woven FRP Laminates, *Journal of Composites Science*, Vol. 5(5), 2021, pp. 115-129, (doi: 10.3390/jcs5050115).
- [4] F. Martinez-Hergueta, D. Ares, A. Ridruejo et al., Modelling the in-plane strain rate dependent behaviour of woven composites with special emphasis on the non-linear shear response, *Composite Structures*, Vol. 210, 2018, pp. 840-857, (doi: 10.1016/j.compstruct.2018.12.002).
- [5] L. Raimondo, L. Iannucci, P. Robinson and P.T. Curtis, Modelling of strain rate effects on matrix dominated elastic and failure properties of unidirectional fibre-reinforced polymer-matrix composites, *Composite Science and Technology*, Vol. 72, 2012, pp. 819-827, (doi: 10.1016/j.compscitech.2012.02.011).
- [6] L. A. Coles, A. Roy, and V. Silberschmidt, Ice Vs. Steel: Ballistic Impact of Woven Carbon/epoxy Composites. Part II – Numerical Modelling, *Engineering Fracture Mechanics*, Vol. 225, 2019, pp. 106297-106314, (doi: 10.1016/j.engfracmech.2018.12.030).
- [7] L. A. Coles, A. Roy, N. Sazhenkov et al., Ice Vs. Steel: Ballistic Impact of Woven Carbon/epoxy Composites. Part I – Deformation and damage behaviour, *Engineering Fracture Mechanics*, Vol. 225, 2019, pp. 106270-106287, (doi: 10.1016/j.engfracmech.2018.12.003).
- [8] J. Hoffmann, *An investigation into the characterisation and modelling of the impact response of CFRP*, Exeter College, University of Oxford, 2018.
- [9] E. Giannaros, A. Kotzakolios, G. Sotiriadis and V. Kostopoulos, A multi-stage material model calibration procedure for enhancing numerical solution fidelity in the case of impact loading of composites, *Journal of composite materials*, Vol. 55(1), 2021, pp. 39-56, (doi: 10.1177/0021998320944992).
- [10] I. M. Daniel, B. T. Werner, J. S. Fenner, Strain-rate-dependent failure criteria for composites, *Composites Science and Technology*, Vol. 71(3), 2011, pp. 357-364, (doi: 10.1016/j.compscitech.2010.11.028).
- [11] X. Hu, J. Tang, W. Xiao and K. Qu, A Strain Rate Dependent Progressive Damage Model for Carbon Fiber Woven Composites under Low Velocity Impact, *2021 The 2nd International Conference on Mechanical Engineering and Materials (ICMEM 2021) 19-20 November 2021, Beijing, China*, Journal of Physics: Conference Series, 2021, Vol. 2101, pp. 012073-012079, (doi: 0.1088/1742-6596/2101/1/012073).
- [12] J. V. Calvo, N. Feito, M. Henar Miguélez, E. Giner, Modeling the delamination failure under compressive loads in CFRP laminates based on digital image correlation analysis, *Composite Structures*, Vol. 287, 2022, pp.115265, (doi: 10.1016/j.compstruct.2022.115265).
- [13] Z. Liu, Y. Xia, and S. Guo, Characterization methods of delamination in a plain woven CFRP composite, *Journal of Material Science*, Vol. 54, 2019, pp. 13157–13174, (doi: 10.1007/s10853-019-03847-4).